

Generating admissible space-time meshes for moving domains in $d + 1$ -dimensions

Elias Karabelas · Martin Neumüller

Abstract In this paper we present a discontinuous Galerkin finite element method for the solution of the transient Stokes equations on moving domains. For the discretization we use an interior penalty Galerkin approach in space, and an upwind technique in time. The method is based on a decomposition of the space-time cylinder into finite elements. Our focus lies on three-dimensional moving geometries, thus we need to triangulate four dimensional objects. For this we will present an algorithm to generate $d + 1$ -dimensional simplex space-time meshes and we show under natural assumptions that the resulting space-time meshes are admissible. Further we will show how one can generate a four-dimensional object resolving the domain movement. First numerical results for the transient Stokes equations on triangulations generated with the newly developed meshing algorithm are presented.

Keywords finite elements · moving domains · four-dimensional mesh generation · parabolic PDE · space-time · discontinuous Galerkin

E. Karabelas
 Medical University of Graz
 Institute of Biophysics
 Harrachgasse 21/IV
 A-8010 Graz, Austria
 Tel.: +43-316-380 7759
 Fax: +43-316-380 9660
 E-mail: elias.karabelas@medunigraz.at

M. Neumüller
 Johannes Kepler University
 Institute of Computational Mathematics
 Altenberger Strasse 69
 A-4040 Linz, Austria

1 Introduction

The finite element approximation of transient partial differential equations is in most cases based on explicit or implicit time discretization schemes. In particular the simultaneous consideration of different time steps requires an appropriate interpolation to couple the solutions at different time levels. Especially for spatial domains with a moving boundary one encounters various numerical difficulties. One usually relies on an arbitrary Lagrangian-Eulerian formulation. See for example the recent article [13] and references therein for an overview of the ongoing discussion. In this paper we consider the application of finite elements in the whole space-time cylinder Q . By this we mean a decomposition of Q into simplicial elements. Therefore one replaces the problem of time discretization by a meshing problem. Having this, one can resolve the possible movement of the domain Ω directly. Simplicial space-time meshes have advantages over tensor-product meshes, since it is easier to decompose complex space-time meshes by those elements.

Space-time finite element methods have been applied to several parabolic model problems. Least square methods for convection-diffusion problems are considered, e.g., in [5, 7] and for flow problems, e.g., in [17, 25, 26, 27, 28, 22]. Discontinuous Galerkin finite element methods have been applied to solve transient convection-diffusion problems in [24], for fluid dynamics see [30] and problems from solid mechanics see [18, 2, 10, 1]. Very recently a paper concerning the generation of 4D simplicial meshes from a sequence of 3D MRI data has been considered in [12]. Also rather recently, the X-FEM method has been considered in the space-time setting see [14]. In most cases, the time dependent equation is discretized in the space-time domain on *space-*

time slabs. This allows for local mesh refinement in the space-time domain, see for example [27].

In this paper we consider, similar to [7], a decomposition of the space-time cylinder into simplicial finite elements. In particular for spatial domains $\Omega \subsetneq \mathbb{R}^3$ the space-time cylinder is a four-dimensional object, which has to be decomposed into finite elements.

In [7], a method based on Delaunay's algorithm is given to construct a four-dimensional triangulation out of a given decomposition of the spatial domain Ω . This method relies on the extension of the given finite elements of the triangulation of Ω to four-dimensional prisms. Afterwards a random perturbation of the resulting points is made, to ensure the admissibility of the resulting four dimensional mesh. Here, we present a different approach using similar ideas. Our method does not rely on random perturbations. Furthermore we can ensure and proof that the resulting mesh is admissible and we can also include movements of the domain boundary. We want to stress out, that our approach is still limited to a special class of boundary movements which we will describe in Section 3.4.

We will consider Stokes flow as a motivating model problem. For the approximation of the transient Stokes equations in the space-time cylinder we consider a discontinuous Galerkin finite element method. In particular, we apply an interior penalty approach in space [3, 6, 23, 21], and an upwind technique in time [29, 19].

This paper is organized as follows. In Section 2 we describe the discontinuous Galerkin finite element method to solve the transient Stokes equations as a model problem. The core part of this paper and the main results are given in Section 3 where we describe our algorithm to generate a four-dimensional triangulation out of a given three-dimensional one. In Section 4 we present some numerical results which underline the applicability of the proposed approach. We close the paper with some conclusions and comments on further work.

2 Space-time discontinuous Galerkin Method

For any $t \in (0, T)$ let $\Omega(t) \subsetneq \mathbb{R}^d$ with $d = 1, 2, 3$ be a bounded Lipschitz domain with boundary $\Gamma(t) := \partial\Omega(t)$. We assume that the boundary $\Gamma(t)$ admits the following decomposition for every $t \in (0, T)$

$$\Gamma(t) = \Gamma_D(t) \cup \Gamma_R(t). \quad (1)$$

We assume that the movement of the domain $\Omega(t)$ is known for every $t \in [0, T]$. We define the space-time cylinder Q as

$$Q := \{(\mathbf{x}, t) \in \mathbb{R}^{d+1} : \mathbf{x} \in \Omega(t) \ t \in (0, T)\}.$$

Further we define the space-time mantle Σ as

$$\Sigma := \{(\mathbf{x}, t) \in \mathbb{R}^{d+1} : \mathbf{x} \in \Gamma(t) \ t \in (0, T)\}.$$

The decomposition (1) induces

$$\Sigma = \Sigma_D \cup \Sigma_R.$$

The model problem we intend to study is governed by the transient Stokes equations. It reads as find (\mathbf{u}, p) such that

$$\begin{aligned} \frac{\partial}{\partial t} \mathbf{u} - \nu \Delta \mathbf{u} + \nabla p &= \mathbf{f} && \text{in } Q, \\ \operatorname{div}(\mathbf{u}) &= 0 && \text{in } Q, \\ \mathbf{u} &= \mathbf{g}_D && \text{on } \Sigma_D, \\ \nabla \mathbf{u} \cdot \mathbf{n} + \alpha_R \mathbf{u} - p \mathbf{n} &= \mathbf{g}_R && \text{on } \Sigma_R, \\ \mathbf{u} &= \mathbf{u}_0 && \text{on } \Sigma_0 := \Omega(0). \end{aligned} \quad (2)$$

Remark 1 In the case of a non-moving domain the definition of Q and Σ simplifies to

$$\begin{aligned} Q &:= \Omega \times (0, T), \\ \Sigma &:= \partial\Omega \times (0, T). \end{aligned}$$

For deriving a discrete variational formulation we need to decompose the space-time cylinder Q into simplicial elements, see [20]. Let \mathcal{T}_h be a sequence of decompositions

$$\overline{Q} = \overline{\mathcal{T}}_h = \bigcup_{k=1}^N \overline{\tau}_k$$

into finite elements of mesh size h_k . For $d = 1$ we have triangles, for $d = 2$ we use tetrahedrons and for $d = 3$ pentatopes are chosen. The generation of such triangulations from a given triangulation of $\Omega(0)$ is not trivial. We will address this topic in Section 3.

Definition 1 (Admissible decomposition) A decomposition \mathcal{T}_h is called *admissible* iff the non-empty intersection of the closure of two finite elements is either an edge (for $d = 1, 2, 3$), a triangle (for $d = 2, 3$) or a tetrahedron (for $d = 3$).

It is worth noting that discontinuous Galerkin methods are not restricted to admissible decompositions. However one needs additional technical assumptions, see [9].

Definition 2 (Interior facet) Let \mathcal{T}_h be a decomposition of Q into finite elements τ_k . For two neighboring elements $\tau_k, \tau_l \in \mathcal{T}_h$ we call

$$\Gamma_{kl} := \overline{\tau}_k \cap \overline{\tau}_l$$

an *interior facet* iff Γ_{kl} is a d -dimensional manifold. The set of all interior facets will be defined as \mathcal{I}_h .

Any interior element Γ_{kl} has an exterior normal vector \mathbf{n}_{kl} with a non-unique direction. We fix the direction of the normal vector such that \mathbf{n}_{kl} is the exterior normal vector of the element τ_k when $k < l$. So the direction of the normal vector \mathbf{n}_{kl} depends on the ordering of the finite elements, but the variational formulation which we are going to use will be independent of this ordering.

Definition 3 Let $\Gamma_{kl} \in \mathcal{I}_h$ be an interior facet with outer normal $\mathbf{n}_k = (\mathbf{n}_{x,k}, n_{t,k})^\top \in \mathbb{R}^{d+1}$ for τ_k and $\mathbf{n}_l = -\mathbf{n}_k$ for τ_l . For a given function ϕ smooth enough restricted to either τ_k or τ_l one defines :

- The *jump* across Γ_{kl} as

$$[[\phi]]_{kl} := \phi|_{\tau_k} \mathbf{n}_k + \phi|_{\tau_l} \mathbf{n}_l.$$

- The *space jump* across Γ_{kl} as

$$[[\phi]]_{\mathbf{x},kl} := \phi|_{\tau_k} \mathbf{n}_{\mathbf{x},k} + \phi|_{\tau_l} \mathbf{n}_{\mathbf{x},l}.$$

- The *time jump* across Γ_{kl} as

$$[[\phi]]_{t,kl} := \phi|_{\tau_k} n_{t,k} + \phi|_{\tau_l} n_{t,l}.$$

- The *average* of ϕ on Γ_{kl} as

$$\langle \phi \rangle_{kl} := \frac{1}{2} (\phi|_{\tau_k} + \phi|_{\tau_l}).$$

- The *upwind* in time direction of ϕ is defined as

$$\{\phi\}_{kl}^{\text{up}} := \begin{cases} \phi|_{\tau_k} & \text{if } n_{k,t} > 0 \\ 0 & \text{if } n_{k,t} = 0 \\ \phi|_{\tau_l} & \text{if } n_{k,t} < 0 \end{cases}$$

Let $p, q \in \mathbb{N}_0$. Then one defines the spaces of piecewise polynomials

$$V_h^p := [S_h^p(\mathcal{T}_h)]^d = \left\{ \mathbf{v}_h \in [L^2(Q)]^d : \mathbf{v}_h|_{\tau_l} \in [\mathbb{P}_p(\tau_l)]^d \text{ for all } \tau_l \in \mathcal{T}_h, \mathbf{v}_h|_{\Sigma_D} = \mathbf{0} \right\},$$

$$Q_h^q := \left\{ q_h \in L^2(Q) : q_h|_{\tau_l} \in \mathbb{P}_q(\tau_l) \text{ for all } \tau_l \in \mathcal{T}_h \right\}.$$

Inspired by works in [19, 21] we will use the following bilinear form defined for $\mathbf{u}_h, \mathbf{v}_h \in V_h^p(\mathcal{T}_h)$:

$$A(\mathbf{u}_h, \mathbf{v}_h) := b_T(\mathbf{u}_h, \mathbf{v}_h) + a_h(\mathbf{u}_h, \mathbf{v}_h).$$

The individual components read as

$$\begin{aligned} a_h(\mathbf{u}_h, \mathbf{v}_h) &:= \nu \sum_{l=1}^N \int_{\tau_l} \nabla_{\mathbf{x}} \mathbf{u}_h : \nabla_{\mathbf{x}} \mathbf{v}_h \, dq \\ &\quad - \nu \sum_{\Gamma_{kl} \in \mathcal{I}_h} \int_{\Gamma_{kl}} \langle \nabla_{\mathbf{x}} \mathbf{u}_h \rangle_{\Gamma_{kl}} [[\mathbf{v}_h]]_{\Gamma_{kl}, \mathbf{x}} \, ds_q \\ &\quad - \nu \sum_{\Gamma_{kl} \in \mathcal{I}_h} \int_{\Gamma_{kl}} \langle \nabla_{\mathbf{x}} \mathbf{v}_h \rangle_{\Gamma_{kl}} [[\mathbf{u}_h]]_{\Gamma_{kl}, \mathbf{x}} \, ds_q, \\ &\quad + \sum_{\Gamma_{kl} \in \mathcal{I}_h} \frac{\sigma_u}{\bar{h}_{kl}} \int_{\Gamma_{kl}} [[\mathbf{u}_h]]_{\Gamma_{kl}, \mathbf{x}} [[\mathbf{v}_h]]_{\Gamma_{kl}, \mathbf{x}} \, ds_q \\ &\quad + \int_{\Sigma_R} \alpha_R(\mathbf{x}, t) \mathbf{u}_h \cdot \mathbf{v}_h \, ds_q, \end{aligned}$$

and

$$\begin{aligned} b_T(\mathbf{u}_h, \mathbf{v}_h) &:= \sum_{l=1}^N - \int_{\tau_l} \mathbf{u}_h \cdot \frac{\partial}{\partial t} \mathbf{v}_h \, dq + \int_{\Sigma_T} \mathbf{u}_h \cdot \mathbf{v}_h \, ds_q \\ &\quad + \sum_{\Gamma_{kl} \in \mathcal{I}_h} \int_{\Gamma_{kl}} \{\mathbf{u}_h\}^{\text{up}} [[\mathbf{v}_h]]_{\Gamma_{kl}, t} \, ds_q \end{aligned}$$

for a given velocity stabilization parameter $\sigma_u > 0$. Furthermore we define the following pressure bilinear forms for $\mathbf{v}_h \in V_h^p(\mathcal{T}_h)$ and $(p_h, q_h) \in Q_h^q(\mathcal{T}_h) \times Q_h^q(\mathcal{T}_h)$:

$$\begin{aligned} b_p(\mathbf{v}_h, p_h) &:= \sum_{l=1}^N \int_{\tau_l} p_h \operatorname{div}(\mathbf{v}_h) \, dq \\ &\quad - \sum_{\Gamma_{kl}} \int_{\Gamma_{kl}} \langle p_h \rangle_{\Gamma_{kl}} [[\mathbf{v}_h]]_{\Gamma_{kl}, \mathbf{x}} \, ds_q, \\ d_p(p_h, q_h) &:= \sum_{\Gamma_{kl} \in \mathcal{I}_h} \sigma_p \bar{h}_{kl} \int_{\Gamma_{kl}} [[p_h]]_{\Gamma_{kl}, \mathbf{x}} [[q_h]]_{\Gamma_{kl}, \mathbf{x}} \, ds_q \end{aligned}$$

for a given pressure stabilization parameter σ_p . In all the bilinear forms defined above we have used $\bar{h}_{kl} := \frac{1}{2}(h_k + h_l)$. Hence we have to find $\mathbf{u}_h^0 \in V_h^p(\mathcal{T}_h)$ and $p_h \in Q_h^q(\mathcal{T}_h)$ such that

$$A(\mathbf{u}_h^0, \mathbf{v}_h) - b_p(\mathbf{v}_h, p_h) = \langle \mathbf{f}, \mathbf{v}_h \rangle_Q + \langle \mathbf{u}_0, \mathbf{v}_h \rangle \quad (3)$$

$$- A(\mathbf{u}_g^h, \mathbf{v}_h), \quad (4)$$

$$b_p(\mathbf{u}_h^0, q_h) + d_p(p_h, q_h) = -b_p(\mathbf{u}_g^h, q_h). \quad (5)$$

Here we used an discrete extension \mathbf{u}_g^h of the given Dirichlet data, for example a L^2 -projection.

3 Triangulations in $d + 1$ dimensions

In this section we will introduce an algorithm to decompose a hyperprism into simplices to generate a $d + 1$ simplex space-time mesh. Moreover we will show that the resulting mesh is admissible if the nodes of the simplices from the initial mesh are sorted in a special way.

3.1 Tensor product extensions

A simple idea for constructing a space-time mesh for a given three-dimensional simplicial spatial mesh is to extrude the mesh in time direction by a tensor product extension, see also Figure 1. Afterwards we decompose the upcoming prisms or so called hyperprisms into simplicial elements.

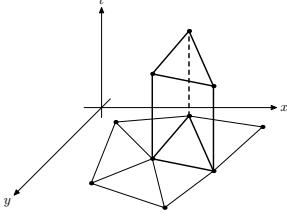


Fig. 1: Tensor extension of a two-dimensional simplex

Before we can start we need a precise definition of a d -dimensional simplex.

Definition 4 (d -dimensional simplex) Let

$$\{\mathbf{p}_1, \dots, \mathbf{p}_{d+1}\} \subset \mathbb{R}^d,$$

$d \in \mathbb{N}$ be a set of nodes, then a d -dimensional simplex S_d is defined as

$$S_d := [\mathbf{p}_1, \dots, \mathbf{p}_{d+1}] := \text{conv}(\{\mathbf{p}_1, \dots, \mathbf{p}_{d+1}\}),$$

where $\text{conv}(\cdot)$ is the convex hull of a set of nodes. Note that we also fix the ordering of the nodes in the definition of a d -dimensional simplex.

Now we can extrude one simplex in time direction and we obtain the following definition.

Definition 5 (Hyperprism) For a given simplex $S_d = [\mathbf{p}_1, \dots, \mathbf{p}_{d+1}]$ the tensor product extension in time direction for a given time interval $[0, \tau]$ or the so called hyperprism H_{d+1} is given by

$$\begin{aligned} P_{d+1} &:= [\mathbf{p}_1, \dots, \mathbf{p}_{d+1}; \tau] \\ &:= \text{conv}(\{\mathbf{p}'_1, \dots, \mathbf{p}'_{d+1}, \mathbf{p}''_1, \dots, \mathbf{p}''_{d+1}\}) \subset \mathbb{R}^{d+1}, \end{aligned}$$

with

$$\mathbf{p}'_i := (\mathbf{p}_i^\top, 0)^\top,$$

$$\mathbf{p}''_i := (\mathbf{p}_i^\top, \tau)^\top,$$

for $i = 1, \dots, d+1$.

3.2 Decomposing Hyperprisms

In this section we will give an algorithm to decompose the hyperprisms given in Definition 5 into simplices.

Definition 6 (Decomposed hyperprism) Let S_d be a given simplex and P_{d+1} the hyperprism with respect to the simplex S_d and $\tau > 0$. Then we define the following simplices

$$\begin{aligned} S_{d+1}^1 &:= [\mathbf{p}'_1, \mathbf{p}'_2, \mathbf{p}'_3, \dots, \mathbf{p}'_{d+1}, \mathbf{p}''_1], \\ S_{d+1}^2 &:= [\mathbf{p}'_2, \mathbf{p}'_3, \dots, \mathbf{p}'_{d+1}, \mathbf{p}''_1, \mathbf{p}''_2], \\ S_{d+1}^3 &:= [\mathbf{p}'_3, \dots, \mathbf{p}'_{d+1}, \mathbf{p}''_1, \mathbf{p}''_2, \mathbf{p}''_3], \\ &\vdots \\ S_{d+1}^{d+1} &:= [\mathbf{p}'_{d+1}, \mathbf{p}''_1, \mathbf{p}''_2, \mathbf{p}''_3, \dots, \mathbf{p}''_{d+1}]. \end{aligned} \tag{6}$$

Furthermore we define the set of simplices $\mathcal{T}_P(S_d, \tau) := \{S_{d+1}^1, \dots, S_{d+1}^{d+1}\}$.

Note, that the ordering of the nodes of a hyperprism P_{d+1} is essential for the resulting decomposition (6). In order to ensure that the simplices $S_{d+1}^1, \dots, S_{d+1}^{d+1}$ defined in (6) decompose the hyperprism P_{d+1} we need the following lemma.

Lemma 1 Let P_{d+1} be some given hyperprism with respect to the simplex S_d and $\tau > 0$. Then the set of simplices

$$\mathcal{T}_P(S_d, \tau) = \{S_{d+1}^1, \dots, S_{d+1}^{d+1}\}$$

defined in (6) is an admissible decomposition of the hyperprism P_{d+1} .

Proof By construction the set of simplices $\mathcal{T}_P(S_d, \tau) = \{S_{d+1}^1, \dots, S_{d+1}^{d+1}\}$ is admissible. Furthermore, every simplex S_{d+1}^i for $i = 1, \dots, d+1$ is contained in the hyperprism P_{d+1} since P_{d+1} is convex. It remains to show, that the union of all simplices $\mathcal{T}_P(S_d, \tau)$ is equal to the hyperprism, i.e. we have to show, that the volume of the union of all simplices $\mathcal{T}_P(S_d, \tau)$ coincides with the volume of the hyperprism. To do so, we transform the hyperprism P_{d+1} to a reference hyperprism \hat{P}_{d+1} where we easily can compute all the volume terms. For this, we define the reference Simplex $\hat{S}_d \subset \mathbb{R}^d$ as

$$\hat{S}_d := [\mathbf{e}_0, \mathbf{e}_1, \dots, \mathbf{e}_d] = \text{conv}(\{\mathbf{e}_0, \mathbf{e}_1, \dots, \mathbf{e}_d\}),$$

with

$$\mathbf{e}_0 := (0, 0, \dots, 0, 0)^\top,$$

$$\mathbf{e}_1 := (1, 0, \dots, 0, 0)^\top,$$

$$\mathbf{e}_2 := (0, 1, \dots, 0, 0)^\top,$$

$$\vdots$$

$$\mathbf{e}_d := (0, 0, \dots, 0, 1)^\top.$$

Then we define the reference hyperprism \hat{P}_{d+1} as

$$\hat{P}_{d+1} := [e_0, \dots, e_{d+1}; 1].$$

With the standard affine transformation we have a bijective mapping between the reference hyperprism \hat{P}_{d+1} and the hyperprism P_{d+1} . This affine transformation consists of the standard transformation for d -dimensional simplices and a scaling in time direction. So we only have to compare the volume for the reference hyperprism. Now the volume of the reference simplex \hat{S}_d is given by $|\hat{S}_d| = \frac{1}{d!}$. Hence the volume of the reference hyperprism is

$$|\hat{P}_{d+1}| = \frac{1}{d!}.$$

The simplices of our decomposition in the reference domain are given by

$$\begin{aligned} \hat{S}_{d+1}^1 &:= [e'_0, e'_1, e'_2, \dots, e'_d, e''_0], \\ \hat{S}_{d+1}^2 &:= [e'_1, e'_2, \dots, e'_d, e''_0, e'_1], \\ \hat{S}_{d+1}^3 &:= [e'_2, \dots, e'_d, e''_0, e'_1, e'_2], \\ &\vdots \\ \hat{S}_{d+1}^{d+1} &:= [e'_d, e''_0, e'_1, e'_2, \dots, e'_d]. \end{aligned}$$

It is easy to see, that these simplices have the same volume, i.e.

$$|\hat{S}_{d+1}^i| = \frac{1}{(d+1)!}, \quad \text{for } i = 1, \dots, d+1.$$

Hence we have

$$\left| \bigcup_{i=1}^{d+1} \hat{S}_{d+1}^i \right| = (d+1) \frac{1}{(d+1)!} = \frac{1}{d!} = |\hat{P}_{d+1}|,$$

which completes the proof.

3.3 Admissible tensor product triangulations

For a given d -dimensional triangulation \mathcal{T}_h we now want to construct a tensor product extension by applying the algorithm (6) for every simplex of the simplicial mesh \mathcal{T}_h . With Lemma 1 we know, that every hyperprism can be decomposed admissible into simplex elements. In this section we want to formulate conditions such that the overall space-time mesh is admissible. For this we need that the nodes of the simplices are ordered in a special way.

Definition 7 (Consistently numbered) Let

$$\mathcal{T}_h = \{S_d^i : S_d^i = [p_1^i, \dots, p_{d+1}^i]\},$$

be an admissible d -dimensional simplex mesh. Then \mathcal{T}_h is called *consistently numbered*, iff for any two simplices $S_d^i, S_d^j \in \mathcal{T}_h$ with non-empty intersection, i.e. $S_d^i \cap S_d^j \neq \emptyset$, there exists indices $k_1 < \dots < k_n$ and $\ell_1 < \dots < \ell_n$ with $n \in \mathbb{N}, n \leq d+1$, such that

$$S_d^i \cap S_d^j = [p_{k_1}^i, \dots, p_{k_n}^i] \equiv [p_{\ell_1}^j, \dots, p_{\ell_n}^j].$$

Here “=” means that the two sets are the same and “ \equiv ” means that the two sets are equal and that also the numbering of the nodes is the same, i.e. $p_{k_1}^i = p_{\ell_1}^j, \dots, p_{k_n}^i = p_{\ell_n}^j$.

The definition of a consistently numbered triangulation can also be found in [8] and it is important for the refinement of d -dimensional simplices, especially for $d \geq 4$. If an admissible mesh is consistently numbered we can prove the next Theorem.

Theorem 1 *Let \mathcal{T}_h be an admissible d -dimensional triangulation which is consistently numbered and let $\tau > 0$. Furthermore let*

$$\mathcal{T}_{h,\tau} := \{\mathcal{T}_P(S_d, \tau) : S_d \in \mathcal{T}_h\}$$

be the $(d+1)$ -dimensional simplex mesh resulting by decomposing every hyperprism with the algorithm given in (6). Then the space-time mesh $\mathcal{T}_{h,\tau}$ is admissible.

Proof With Lemma 1 we know, that every hyperprism is decomposed admissible into simplices. To obtain a global admissible mesh we have to prove, that the tensor product triangulations $\mathcal{T}_P(S_d^i, \tau)$ and $\mathcal{T}_P(S_d^j, \tau)$ for each neighboring elements $S_d^i, S_d^j \in \mathcal{T}_h$ are matching. Let

$$S_d^i = [p_1^i, \dots, p_{d+1}^i] \quad \text{and} \quad S_d^j = [p_1^j, \dots, p_{d+1}^j]$$

with $S_d^i, S_d^j \in \mathcal{T}_h$ be some neighboring simplices and

$$P_d := P_{d+1}^i \cap P_{d+1}^j,$$

with

$$P_{d+1}^i := [p_1^i, \dots, p_{d+1}^i; \tau] \quad \text{and} \quad P_{d+1}^j := [p_1^j, \dots, p_{d+1}^j; \tau]$$

be the intersecting hyperprism and

$$\mathcal{T}_P^i := \{S_{d+1} \cap P_d : S_{d+1} \in \mathcal{T}_P(S_d^i, \tau)\},$$

$$\mathcal{T}_P^j := \{S_{d+1} \cap P_d : S_{d+1} \in \mathcal{T}_P(S_d^j, \tau)\},$$

be the corresponding triangulations of P_d obtained by $\mathcal{T}_P(S_d^i, \tau)$ and $\mathcal{T}_P(S_d^j, \tau)$. It remains to show, that the intersecting hyperprism P_d is decomposed in the same way from both sides, i.e. that $\mathcal{T}_P^i = \mathcal{T}_P^j$. Since \mathcal{T}_h is

consistently numbered, there exists indices $k_1 < \dots < k_n$ and $\ell_1 < \dots < \ell_n$ with $n = d$, such that

$$\begin{aligned} S_d^i \cap S_d^j &= S_{d-1}^i := [\mathbf{p}_{k_1}^i, \dots, \mathbf{p}_{k_n}^i] \\ &\equiv S_{d-1}^j := [\mathbf{p}_{\ell_1}^j, \dots, \mathbf{p}_{\ell_n}^j]. \end{aligned} \quad (7)$$

Therefore, the intersecting simplex $S_d^i \cap S_d^j$ is obtained by simply removing the nodes from S_d^i or S_d^j which are not shared together and furthermore they have the same ordering of the nodes. For the intersecting hyperpism P_d the decompositions from both sides \mathcal{T}_P^i and \mathcal{T}_P^j are given by removing the nodes which are not shared together from the formula (6) and with (7) we have

$$\mathcal{T}_P^i = \mathcal{T}_P(S_{d-1}^i, \tau) \quad \text{and} \quad \mathcal{T}_P^j = \mathcal{T}_P(S_{d-1}^j, \tau).$$

Since in equation (7) also the node ordering of S_{d-1}^i and S_{d-1}^j is the same we also obtain

$$\mathcal{T}_P(S_{d-1}^i, \tau) = \mathcal{T}_P(S_{d-1}^j, \tau),$$

which implies that $\mathcal{T}_P^i = \mathcal{T}_P^j$.

Remark 2 To obtain an admissible space-time mesh $\mathcal{T}_{h,\tau}$ we only have to ensure, that the nodes of the spatial mesh \mathcal{T}_h are consistently numbered. This can be easily obtained by sorting for each simplex $S_d \in \mathcal{T}_h$ the local nodes with respect to the global node numbers.

3.4 Tensor product triangulations for moving domains

If the movement of a computational domain is known in advance we can generate admissible space-time meshes by applying the methods from above. The idea is to move the points at the top of the tensor-product extension. Assuming that the displacement of points on the boundary $\Gamma(t)$ is governed by a function

$$\mathbf{g}_{\text{mov}}(\mathbf{X}, t): \Gamma(0) \times (0, T) \rightarrow \mathbb{R}^d.$$

Then a point $\mathbf{x} \in \Gamma(t)$ can be written as

$$\mathbf{x} = \mathbf{X} + \mathbf{g}_{\text{mov}}(\mathbf{X}, t),$$

where $\mathbf{X} \in \Gamma(0)$. Recall the definition of a hyperprism in Definition 5. Instead of using $\mathbf{p}_i'' := (\mathbf{p}_i^\top, \tau)^\top$ on the surface we can apply the displacement and use $\mathbf{p}_i'' := (\mathbf{p}_i^\top + \mathbf{g}_{\text{mov}}(\mathbf{p}_i, \tau)^\top, \tau)^\top$ for all boundary points of the simplex mesh that are subject to a movement. The remaining generation of the 4D mesh stays untouched. For boundary movements that are of small magnitude and do not change the topology of the initial geometry this can be sufficient. For stronger yet topology preserving movements this concept would create degenerating simplex elements. A remedy to this is to use the movement \mathbf{g}_{mov} as Dirichlet datum for a vector Laplacian or

a linear elasticity problem. Then the resulting displacement is applied to all simplex points in the domain. For more on mesh smoothing we refer to [16, 15].

In the case of stronger displacements or even topology changes re-meshing would be required and we need further meshing algorithms to connect different spatial domains in space and time, especially for four-dimensional space-time meshes this remains a future research topic.

If the the movement of the computational domain is not known in advance we can solve the problem on a coarse spatial grid with coarse time steps to obtain a coarse approximation for the movement. Afterwards we can construct the coarse space-time mesh with the methods given in this work. By using adaptive schemes in space and time we further can refine the space-time domain adaptively and move the points in the space time domain by the computed finer approximations. Note that the movement of the points has to be only done in the range of the approximation error, which is usually small. Of course this is also considered as a further research topic.

3.5 Visualization

Here we want to address the issue of visualizing results for four-dimensional triangulations \mathcal{T}_h . In applications it is desired to visualize results at given time instances $t_k \in [0, T]$. The main idea is to cut the decomposition \mathcal{T}_h into a finite number of three-dimensional manifolds. For this we need to have a hyperplane to calculate the intersections with the decomposition.

Definition 8 (Hyperplane) Let $\mathbf{p}_0 \in \mathbb{R}^4$ be arbitrary and let $\mathbf{p}_1, \mathbf{p}_2, \mathbf{p}_3$ and $\mathbf{p}_4 \in \mathbb{R}^4$ be linear independent. Then the set

$$\begin{aligned} H_4 := \{ \mathbf{x} \in \mathbb{R}^4 : \mathbf{x} = \mathbf{p}_0 + \mu_1 \mathbf{p}_1 + \mu_2 \mathbf{p}_2 + \mu_3 \mathbf{p}_3 \\ \text{for } \mu_1, \mu_2, \mu_3 \in \mathbb{R} \} \end{aligned}$$

is called a *hyperplane*.

To cut a given decomposition \mathcal{T}_h with a hyperplane H_4 , we have to cut every element $\tau_k \in \mathcal{T}_h$ with the hyperplane. For this we have to calculate for every edge $e_i = (\mathbf{x}_{i_1}, \mathbf{x}_{i_2})$, $i = 1, \dots, 10$ of τ_k , the intersection with the hyperplane. A point $\mathbf{x} \in e_i$ can be written as

$$\mathbf{x} = \mathbf{x}_{i_1} + \lambda (\mathbf{x}_{i_2} - \mathbf{x}_{i_1})$$

for a given $\lambda \in [0, 1]$. Hence, an intersection point $\boldsymbol{\xi}_i$ of the edge e_i with the hyperplane H_4 has to satisfy

$$\mathbf{x}_{i_1} + \lambda (\mathbf{x}_{i_2} - \mathbf{x}_{i_1}) = \mathbf{p}_0 + \mu_1 \mathbf{p}_1 + \mu_2 \mathbf{p}_2 + \mu_3 \mathbf{p}_3$$

or in matrix notation

$$\mathbf{A}_i := (\mathbf{p}_1 \ \mathbf{p}_2 \ \mathbf{p}_3 \ \mathbf{x}_{i_1} - \mathbf{x}_{i_2}) \begin{pmatrix} \mu_1 \\ \mu_2 \\ \mu_3 \\ \lambda \end{pmatrix} = \mathbf{x}_{i_1} - \mathbf{p}_0.$$

The matrix \mathbf{A}_i is invertible iff the vector $\mathbf{x}_{i_1} - \mathbf{x}_{i_2}$ is linear independent to the vectors $\mathbf{p}_1, \mathbf{p}_2, \mathbf{p}_3$. In fact, the matrix \mathbf{A}_i is not invertible if the edge e_i is parallel to the hyperplane H_4 . In this case there exists either no intersection point or infinitely many. If the matrix is invertible we can calculate the coefficients μ_1, μ_2, μ_3 and $\lambda \in \mathbb{R}$ uniquely. Let D_k denote the set of all intersection points of the element $\tau_k \in \mathcal{T}_h$ with the hyperplane H_4 . We distinguish two relevant cases

1. If $|D_k| = 4$, then the intersection points form a tetrahedron
2. If $|D_k| = 6$, then the intersection points form a general irregular prism.

If we use the special vectors

$$\mathbf{p}_0 := t_* \mathbf{e}_t, \ \mathbf{p}_1 := \mathbf{e}_x, \ \mathbf{p}_2 := \mathbf{e}_y, \ \mathbf{p}_3 := \mathbf{e}_z$$

for a given $t_* \in [0, T]$ we can now calculate a three-dimensional object which can be visualized with existing software tools for example [4].

4 Numerical Results

In this section we will present first numerical examples. Starting point is the discrete variational formulation (3)-(5). This can be equivalently written as the following block system

$$\begin{pmatrix} \mathbf{K}_h & -\mathbf{B}_h^\top \\ \mathbf{B}_h & \mathbf{D}_h \end{pmatrix} \begin{pmatrix} \mathbf{U} \\ \mathbf{P} \end{pmatrix} = \begin{pmatrix} \mathbf{F}_1 \\ \mathbf{F}_2 \end{pmatrix}. \quad (8)$$

It is worth noting, that due to the discretization of the time derivative we have that $\mathbf{K}_h \neq \mathbf{K}_h^\top$. The four dimensional computational geometries as well as the resulting linear systems in the subsequent numerical examples were solved with the software package NESHMET developed by the authors. In particular we used a preconditioned GMRes method. As preconditioner we used the following:

$$\mathbf{P} := \begin{pmatrix} \overline{\mathbf{K}}_h & \\ & \overline{\mathbf{S}}_h \end{pmatrix} \quad (9)$$

where $\overline{\mathbf{K}}_h$ is chosen as a component-wise algebraic multi-grid and $\overline{\mathbf{S}}_h$ is chosen as ILU(2)-factorization of $\mathbf{D}_h + \mathbf{B}_h \text{diag}(\mathbf{K}_h)^{-1} \mathbf{B}_h^\top$. These preconditioners were taken from the HYPRE library [11].

4.1 Robin Boundary Conditions for Simulating Valves

In the subsequent examples we want to simulate opening and closing valves. This means, that we need to switch between an inflow and a no-slip condition. To this end we used the following configuration for (2): We set $\mathbf{g}_R \equiv \mathbf{0}$. Further we use the following Robin coefficients for outflow

$$\alpha_R(x, t) := \begin{cases} 10^6 & \text{if } t \in [0, \frac{1}{2}) \\ 0 & \text{if } t \in [\frac{1}{2}, 1] \end{cases},$$

and the following for inflow:

$$\alpha_R(x, t) := \begin{cases} 0 & \text{if } t \in [0, \frac{1}{2}) \\ 10^6 & \text{if } t \in [\frac{1}{2}, 1] \end{cases}.$$

4.2 First Example

In the first example we consider Stokes flow in a diaphragm pump. The geometry consists of the intersection of two cylinders. The first one has its main axis aligned with the z -axis with a radius of 0.8 and ranges between $z = -0.4$ and $z = 0.4$. The second cylinder has its main axis aligned with the x -axis with a radius of 0.2 and ranges from $x = -1$ to $x = 1$. A front view of the geometry is depicted in Figure 2. The movement of

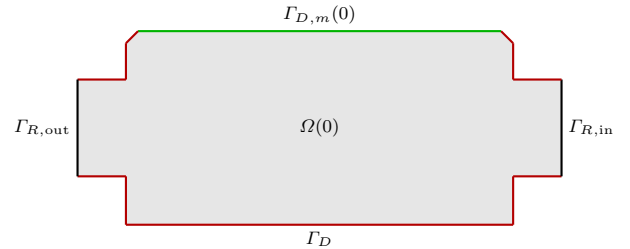


Fig. 2: Front view of the initial geometry $\Omega(0)$. Blue boundaries belong to Γ_D .

the boundary $\Gamma(t)$ was prescribed as follows

$$\mathbf{g}_{\text{mov}}(t, \mathbf{X}) := \left(0.4 + \sin^2(\pi t) \left(1 - \frac{X(0)^2 + X(1)^2}{0.75^2} \right) \right) \mathbf{e}_z - \mathbf{X}$$

for $\mathbf{X} \in \Gamma_{D,m}(0)$ and $\mathbf{0}$ else. The following boundary conditions are used:

- $\mathbf{u} = \mathbf{0}$ on Γ_D
- $\mathbf{u} = \frac{\partial}{\partial t} \mathbf{g}_{\text{mov}}$ on $\Gamma_{D,m}(t)$
- On $\Gamma_{R,\text{in}}$ and $\Gamma_{R,\text{out}}$ we used the Robin boundary conditions discussed in Section 4.1

- The initial condition for \mathbf{u} was set to $\mathbf{u}(0, \mathbf{x}) = \mathbf{0}$.

The triangulation of the resulting 4D geometry was accomplished using the tools described in Section 3. The resulting mesh consisted of 951360 pentatopes.

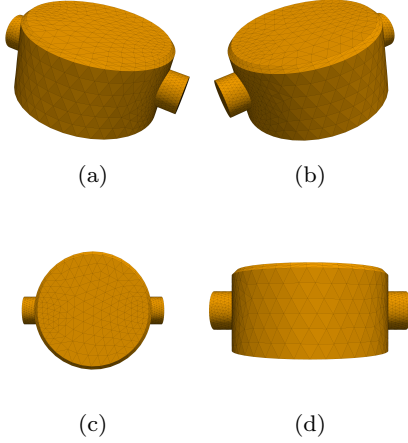


Fig. 3: Initial Triangulation $\Omega(0)$

Some snapshots of the triangulation of the moving domain are depicted in Figure 4. These snapshots were generated by slicing through the 4D mesh along the time axis as described in Section 3.5. The polynomial

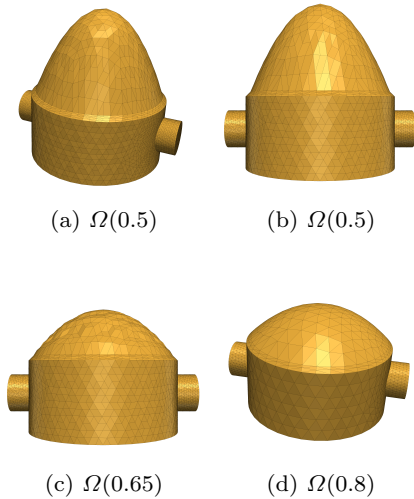


Fig. 4: Snapshots of the Triangulations $\Omega(t)$

degree for \mathbf{u}_h was set to $p = 1$ and $q = 0$ for the pressure variable p_h . This resulted in 14270400 degrees of freedom for \mathbf{u}_h and 951360 degrees of freedom for p_h . We

needed 95 GMRes-iterations for achieving a relative error of $1E - 5$. In Figure 5 one can see the resulting flow and pressure at given time stamps, which were again produced by slicing the 4D geometry along the time axis.

4.3 Second Example

For the second example we considered a Y-shaped pipe. A schematic view is depicted in Figure 2. We prescribed the following movement of $\Gamma(t)$:

$$\mathbf{g}_{\text{mov}}(\mathbf{X}, t) := \begin{cases} \mathbf{0} & \text{for } \mathbf{X} \notin \Gamma_{D,m} \cup \widetilde{\Gamma_{D,m}} \\ 4 \frac{|X(2)+3|}{7} \sin(\pi t)^2 \mathbf{e}_z & \text{for } \mathbf{X} \in \Gamma_{D,m} \cup \widetilde{\Gamma_{D,m}} \end{cases}.$$

Some snapshots of the domain movement are depicted in Figure 8. The boundary conditions were set to

- $\mathbf{u} = \mathbf{0}$ on $\Gamma_D \cup \widetilde{\Gamma_{D,m}}(t)$
- $\mathbf{u} = \frac{\partial}{\partial t} \mathbf{g}_{\text{mov}}$ on $\Gamma_{D,m}(t)$
- On $\Gamma_{R,\text{in}}$ and $\Gamma_{R,\text{out}}$ we used the Robin boundary conditions discussed in Section 4.1
- The initial condition for \mathbf{u} was set to $\mathbf{u}(0, \mathbf{x}) = \mathbf{0}$.

The resulting 4D mesh consisted of 2618880 pentatopes. With the same ansatz spaces as used for Example 1 we have 39283200 degrees of freedom for \mathbf{u}_h and 2618880 degrees of freedom for p_h . We needed 107 GMRes-iterations for achieving a relative error of $1E - 5$. In Figure 9 we have depicted some results.

5 Conclusions

In this paper we have presented a novel approach to construct four-dimensional triangulations for moving domains. This was done by extending the elements of the space triangulation into hyperprisms. Assuming a consistent numbered spatial triangulation we were able to prove that our algorithm produces admissible space-time meshes. We implemented the presented algorithm and applied it to solve the transient Stokes equations with a space-time discontinuous Galerkin finite element method. In the future one could start investigating Navier-Stokes equations. Furthermore, optimal control problems with time dependent partial differential equations render themselves interesting candidates for applying space-time methods, since one has to solve a forward and backward problem which are coupled in space and time. Another attractive aspect of general space-time meshes is the possibility to apply adaptive refinement strategies to resolve local behaviors in space and time. Considering solvers, one could think about domain decomposition approaches or space-time multigrid methods for example, which are a future research topic.

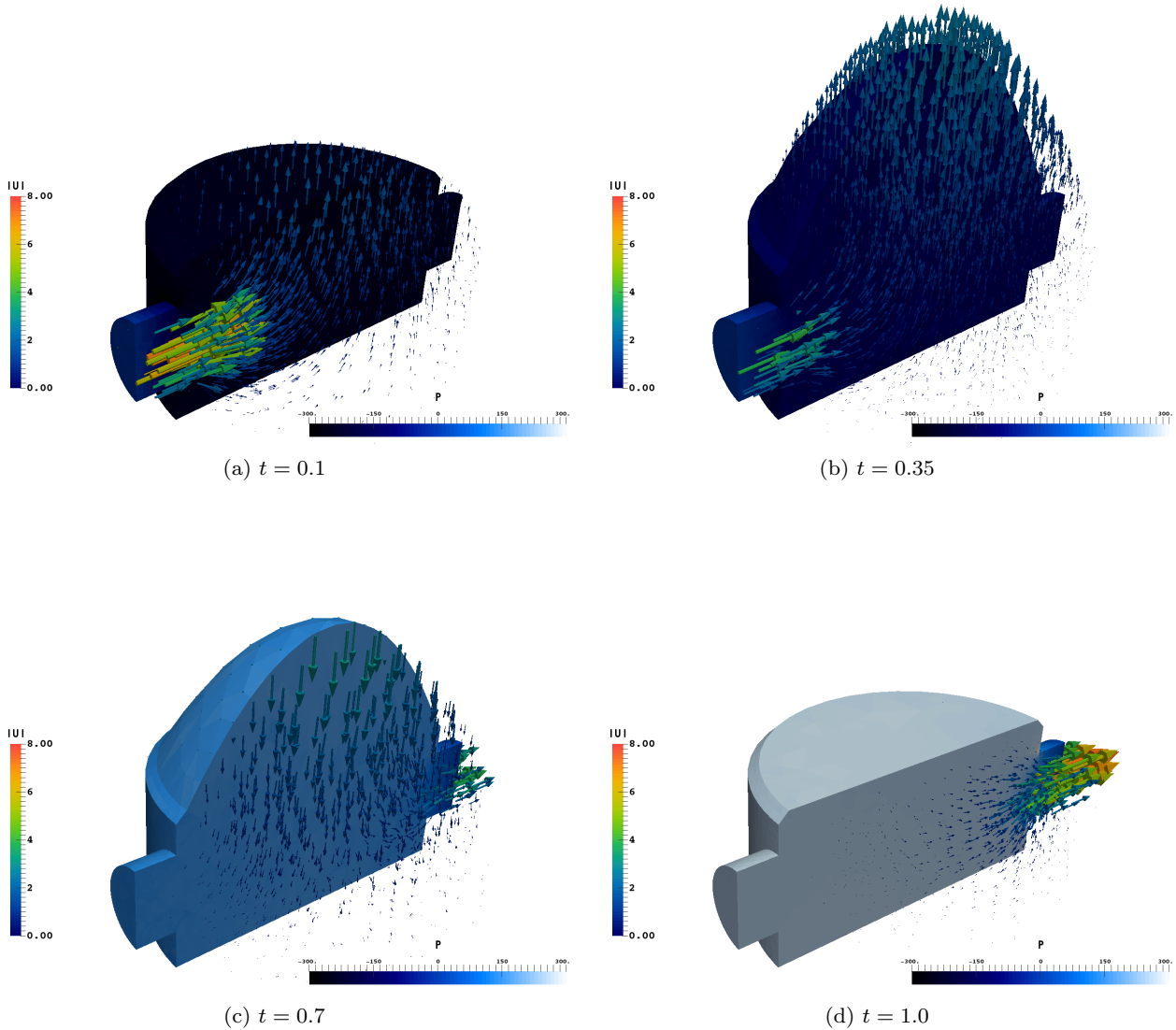


Fig. 5: Snapshots of the solution. Additionally we have cut along the y -axis.

Acknowledgments

This research was supported by the grant F3210-N18 from the Austrian Science Fund (FWF).

References

1. Abedi, R., Hawker, M., Haber, R., Matouš, K.: An adaptive spacetime discontinuous Galerkin method for cohesive models of elastodynamic fracture. *Internat. J. Numer. Methods Engrg.* **81**, 1207–1241 (2010)
2. Abedi, R., Petracovici, B., Haber, R.B.: A space-time discontinuous galerkin method for linearized elastodynamics with element-wise momentum balance. *Computer Methods in Applied Mechanics and Engineering* **195**(25), 3247–3273 (2006)
3. Arnold, D., Brezzi, F., Cockburn, B., Marini, L.: Unified Analysis of Discontinuous Galerkin Methods for Elliptic Problems. *SIAM J. Numer. Anal.* **39**, 1749–1779 (2002)
4. Ayachit., U.: *The ParaView Guide: A Parallel Visualization Application*. Kitware Inc., Clifton Park (2015)
5. Bank, R., Metti, M.: An error analysis of some higher order space-time moving finite elements. *Computing and Visualization in Science* **16**(5), 219–229 (2013). DOI 10.1007/s00791-015-0235-1. URL <http://dx.doi.org/10.1007/s00791-015-0235-1>
6. Baumann, C., Oden, J.: A discontinuous hp finite element method for convection-diffusion problems. *Comput. Methods Appl. Mech. Engrg.* **175**, 311–341 (1999)
7. Behr, M.: Simplex space-time meshes in finite element simulations. *Internat. J. Numer. Methods Fluids* **57**, 1421–1434 (2008)
8. Bey, J.: Simplicial grid refinement: on Freudenthal’s algorithm and the optimal number of congruence classes.

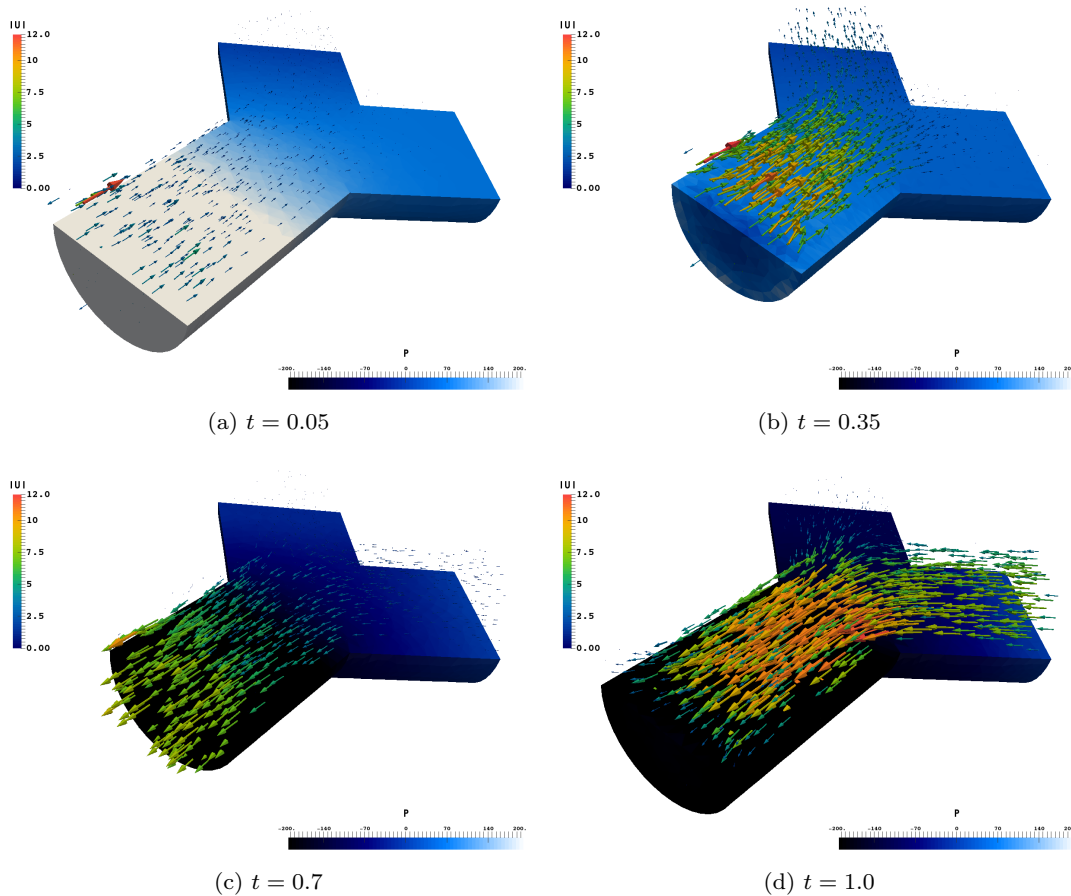


Fig. 9: Snapshots of the solution. Additionally we have cut along the y -axis.

- Numer. Math. **85**, 1–29 (2000)
9. Buffa, A., Ortner, C.: Compact embeddings of broken Sobolev spaces and applications. *IMA J. Numer. Anal.* **29**(4), 827–855 (2009). DOI 10.1093/imanum/drn038. URL <http://dx.doi.org/10.1093/imanum/drn038>
10. Dumont, S., Jourdan, F.: A space-time finite element method for elastodynamics problems with a moving loading zone. In: *CST 2012* (2012)
11. Falgout, R., Jones, J., Yang, U.: The design and implementation of hypre, a library of parallel high performance preconditioners. *Lect. Notes Comput. Sci. Eng.* **51**, 267–294 (2006)
12. Foteinos, P., Chrisochoides, N.: 4d space-time delaunay meshing for medical images. In: *Proceedings of the 22nd International Meshing Roundtable*, pp. 223–240. Springer (2014)
13. Gawlik, E.S., Lew, A.J.: High-order finite element methods for moving boundary problems with prescribed boundary evolution. *Computer Methods in Applied Mechanics and Engineering* **278**, 314–346 (2014)
14. Lehrenfeld, C.: The nitsche xfem-dg space-time method and its implementation in three space dimensions. *SIAM Journal on Scientific Computing* **37**(1), A245–A270 (2015)
15. Liakopoulos, P.I., Giannakoglou, K.C.: Unstructured remeshing using an efficient smoothing scheme approach. In: *ECCOMAS CFD 2006: Proceedings of the European Conference on Computational Fluid Dynamics*, Egmond aan Zee, The Netherlands, September 5–8, 2006. Delft University of Technology; European Community on Computational Methods in Applied Sciences (ECCOMAS) (2006)
16. López, E.J., Nigro, N.M., Storti, M.A.: Simultaneous untangling and smoothing of moving grids. *International journal for numerical methods in engineering* **76**(7), 994–1019 (2008)
17. Masud, A., Hughes, T.: A space-time Galerkin/least-squares finite element formulation of the Navier-Stokes equations for moving domain problems. *Comput. Methods Appl. Mech. Engrg.* **146**, 91–126 (1997)
18. Miller, S.T., Kraczek, B., Haber, R.B., Johnson, D.D.: Multi-field spacetime discontinuous galerkin methods for linearized elastodynamics. *Computer Methods in Applied Mechanics and Engineering* **199**(1), 34–47 (2009)
19. Neumüller, M.: Space-time methods: Fast solvers and applications. Ph.D. thesis, University of Graz (2013)
20. Neumüller, M., Steinbach, O.: A DG space-time domain decomposition method. *Domain Decomposition Methods in Science and Engineering XX* (2013)
21. Di Pietro, D., Ern, A.: *Mathematical Aspects of Discontinuous Galerkin Methods*. Springer, Berlin, Heidelberg (2012)
22. Rendall, T., Allen, C.B., Power, E.D.: Conservative unsteady aerodynamic simulation of arbitrary boundary motion using structured and unstructured meshes in

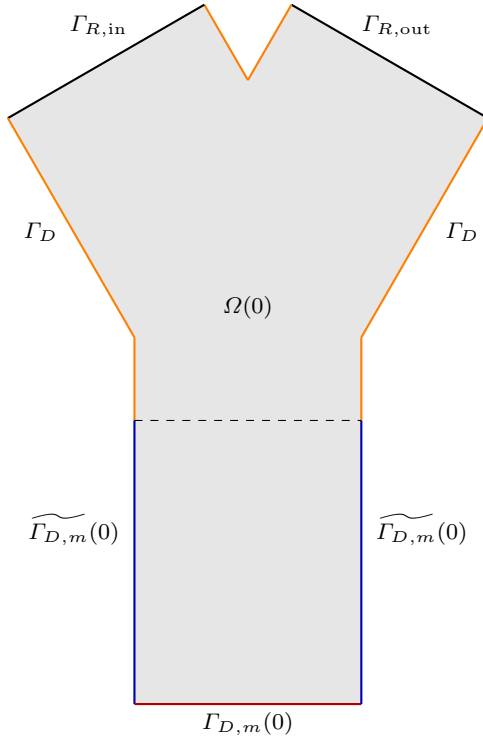


Fig. 6: Front view of the initial geometry $\Omega(0)$. Blue boundaries belong to Γ_D . The dashed line represents the plane $z = -3$. The height from top to bottom is 17. The base of the pipe is located at $z = -10$. The radius of the pipe is 3.

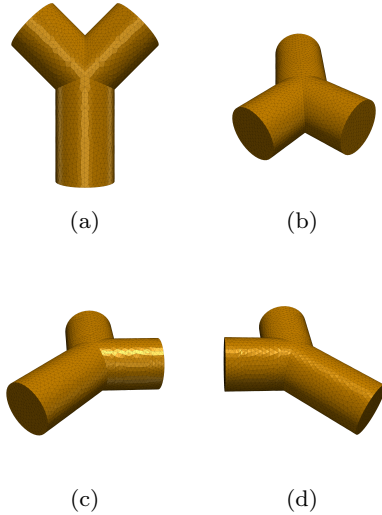


Fig. 7: Initial Triangulation $\Omega(0)$

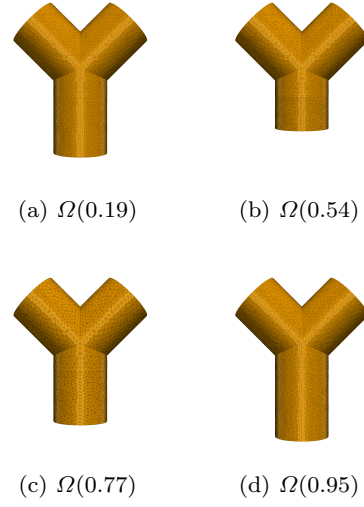


Fig. 8: Snapshots of the Triangulations $\Omega(t)$

- time. *International Journal for Numerical Methods in Fluids* **70**(12), 1518–1542 (2012)
23. Rivière, B.: *Discontinuous Galerkin Methods for Solving Elliptic and Parabolic Equations*. Cambridge University Press (2008)
 24. Sudirham, J., van der Vegt, J., van Damme, R.: Space-time discontinuous Galerkin method for advection-diffusion problems on time-dependent domains. *Appl. Num. Math.* **56**, 1491–1518 (2006)
 25. Tezduyar, T., Behr, M., Liou, J.: A new strategy for finite element computations involving moving boundaries and interfaces: the deforming-spatial-domain/space-time procedure. i: The concept and the preliminary numerical tests. *Computer Methods in Applied Mechanics and Engineering* **94**(3), 339–351 (1992)
 26. Tezduyar, T., Behr, M., Mittal, S., Liou, J.: A new strategy for finite element computations involving moving boundaries and interfaces: the deforming-spatial-domain/space-time procedure: II. computation of free-surface flows, two-liquid flows, and flows with drifting cylinders. *Computer methods in applied mechanics and engineering* **94**(3), 353–371 (1992)
 27. Tezduyar, T., Sathe, S.: Enhanced-discretization space-time technique (EDSTT). *Comput. Methods Appl. Mech. Engrg.* **193**, 1385–1401 (2004)
 28. Tezduyar, T.E.: Interface-tracking and interface-capturing techniques for finite element computation of moving boundaries and interfaces. *Computer Methods in Applied Mechanics and Engineering* **195**(23), 2983–3000 (2006)
 29. Thomée, V.: *Galerkin Finite Element Methods for Parabolic Problems*. Springer, New York (2006)
 30. van der Vegt, J., Sudirham, J.: A space-time discontinuous galerkin method for the time-dependent oseen equations. *Applied Numerical Mathematics* **58**(12), 1892–1917 (2008)